Electronic Supplementary Material (ESI) for Dalton Transactions

Supplementary Information (ESI)

Substitution versus redox reactions of gold(III) complexes with L-cysteine, L-methionine and glutathione

Mirjana D. Đurović,[a] Živadin D. Bugarčić,[a,*] Frank W. Heinemann[b] and Rudi van Eldik[b,*]

[a]*Department of Chemistry, Faculty of Science, University of Kragujevac, R. Domanovića 12,*

P O Box 60, 34000 Kragujevac, Serbia

[c]*Inorganic Chemistry, Department of Chemistry and Pharmacy, University of Erlangen-Nürnberg, Egerlandstr. 1, 91058 Erlangen, Germany*

Table S1. Observed *pseudo*-first order rate constants as a function of nucleophile concentration and chloride concentration in the reaction between $[AuCl_4]^-$ and L-Cys at pH 2.5 (0.003 M $HClO_4$), 298 K.

λ/nm	$10^3\ C_{Cl^-}$/M	$10^3\ C_{L\text{-}Cys}$/M	k_{obsd}/s^{-1}
280	0	2	0.44(10)[a]
		4	0.86(10)
		6	1.27(9)
		8	1.68(9)
		10	2.09(10)
270	10	2	2.06(10)
		4	4.33(9)
		6	6.26(10)
		8	8.70(9)
		10	10.29(10)

[a]Number of runs in parentheses

Table S2. Observed *pseudo*-first order rate constants as a function of nucleophile concentration and chloride concentration in the reaction between $[AuCl_4]^-$ and L-Met at pH 2.5 (0.003 M $HClO_4$), 298 K.

λ/nm	$10^3\ C_{Cl^-}$/M	$10^3\ C_{L\text{-}Met}$/M	k_{obsd}/s^{-1}
270	0	2	2.88(10)
		4	3.64(10)
		6	4.48(10)
		8	5.16(9)
		10	6.04(10)
315	10	2	5.44(9)
		4	13.10(10)
		6	15.70(10)
		8	24.16(9)
		10	28.15(9)

Table S3. Observed *pseudo*-first order rate constants as a function of nucleophile concentration and chloride concentration in the reaction between $[AuCl_4]^-$ and GSH at pH 2.5 (0.003 M $HClO_4$), 298 K.

λ/nm	$10^3\ C_{Cl^-}$/M	$10^3\ C_{GSH}$/M	k_{obsd}/s^{-1}
280	0	2	0.26(10)
		4	0.48(10)
		6	0.60(10)
		6	0.73(9)
		10	0.79(8)
270	10	2	1.89(9)
		4	4.32(9)
		6	6.58(9)
		8	8.31(10)
		10	10.35(9)

Table S4. Observed *pseudo*-first order rate constants as a function of nucleophile concentration and chloride concentration in the reaction between $[AuCl_4]^-$ and L-Cys at pH 7 (0.1 M $NaClO_4$), 298 K.

λ/nm	$10^3\ C_{Cl^-}$/M	$10^3\ C_{L\text{-}Cys}$/M	k_{obsd}/s^{-1}
300	0	2	0.43(9)
		4	0.90(10)
		6	1.49(10)
		8	1.85(8)
		10	2.24(10)
270	10	2	28.80(10)
		4	55.17(10)
		6	89.25(10)
		8	119.9(10)
		10	141.5(10)

Table S5. Observed *pseudo*-first order rate constants as a function of nucleophile concentration and chloride concentration in the reaction between $[AuCl_4]^-$ and L-Met at pH 7 (0.1 M $NaClO_4$), 298 K.

λ/nm	$10^3\ C_{Cl^-}$/M	$10^3\ C_{L\text{-}Met}$/M	k_{obsd}/s^{-1}
270	0	2	1.80(10)
		4	3.04(9)
		6	4.01(8)
		8	5.05(8)
		10	5.97(9)
270	10	2	6.51(10)
		4	8.73(9)
		6	12.34(9)
		8	15.59(9)
		10	19.66(10)

Table S6. Observed *pseudo*-first order rate constants as a function of nucleophile concentration and chloride concentration in the reaction between $[AuCl_4]^-$ and GSH at pH 7 (0.1 M $NaClO_4$), 298 K.

λ/nm	$10^3\ C_{Cl^-}$/M	$10^3 C_{GSH}$/M	k_{obsd}/s^{-1}
300	0	2	0.15(9)
		4	0.31(10)
		6	0.47(9)
		8	0.62(9)
		10	0.73(10)
270	10	2	4.65(10)
		4	8.40(10)
		6	12.90(10)
		8	18.20(8)
		10	21.65(9)

Table S7. Observed *pseudo*-first order rate constants as a function of nucleophile concentration and chloride concentration in the reaction between $[Au(terpy)Cl]^{2+}$ and L-Cys at pH 2.5 (0.003 M $HClO_4$), 298 K.

λ/nm	$10^3\ C_{Cl^-}$/M	$10^3 C_{L\text{-}Cys}$/M	k_{obsd}/s^{-1}
360	0	2	15.75(10)
		4	29.95(10)
		6	46.73(10)
		8	64.34(9)
		10	73.73(9)
360	10	2	10.46(9)
		4	21.68(9)
		6	32.81(9)
		8	43.89(9)
		10	53.23(10)
360	100	2	9.01(9)
		4	18.39(9)
		6	27.00(9)
		8	35.87(10)
		10	44.45(10)

Table S8. Observed *pseudo*-first order rate constants as a function of nucleophile concentration and chloride concentration in the reaction between $[Au(terpy)Cl]^{2+}$ and GSH at pH 2.5 (0.003 M $HClO_4$), 298 K.

λ/nm	$10^3\ C_{Cl^-}$/M	$10^3\ C_{GSH}$/M	k_{obsd}/s^{-1}
360	0	2	5.76(10)
		4	11.94(10)
		6	18.33(9)
		8	25.36(10)
		10	29.19(10)
360	10	2	4.97(10)
		4	9.02(8)
		6	15.53(9)
		8	20.54(10)
		10	23.70(10)
360	100	2	3.49(10)
		4	7.01(10)
		6	11.98(9)
		8	15.16(9)
		10	17.92(10)

Table S9. Observed *pseudo*-first order rate constants as a function of nucleophile concentration and chloride concentration in the reaction between $[Au(terpy)Cl]^{2+}$ and L-Cys at pH = 7 (25 mM Hepes buffer), 298 K.

λ/nm	10^3 C_{Cl^-}/M	10^3 $C_{L\text{-}Cys}$/M	k_{obsd}/s^{-1}
360	0	2	124.70(10)
		4	154.40(10)
		6	190.80(9)
		8	221.70(9)
		10	239.40(8)
370	10	2	158.60(10)
		4	205.50(10)
		6	247.70(9)
		8	281.50(9)
		10	325.90(9)

Table S10. Observed *pseudo*-first order rate constants as a function of nucleophile concentration and chloride concentration in the reaction between $[Au(terpy)Cl]^{2+}$ and L-Met at pH 7 (25 mM Hepes buffer), 298 K.

λ/nm	$10^3\ C_{L\text{-}Met}$/M	$10^4\ k_{obsd}/s^{-1}$
360	2	1.10(4)
	4	1.83(4)
	6	2.17(4)
	8	2.64(4)
	10	2.86(5)

Table S11. Observed *pseudo*-first order rate constants as a function of nucleophile concentration and chloride concentration in the reaction between $[Au(terpy)Cl]^{2+}$ and GSH at pH 7 (25 mM Hepes buffer), 298 K.

λ/nm	10^3 C_{Cl^-}/M	10^3 C_{GSH}/M	k_{obsd}/s^{-1}
370	0	2	14.15(10)
		4	19.87(10)
		6	26.16(9)
		8	31.15(9)
		10	34.76(10)
370	10	2	56.87(10)
		4	70.45(10)
		6	85.19(9)
		8	99.66(9)
		10	109.30(9)
370	100	2	39.90(10)
		4	57.35(10)
		6	71.66(10)
		8	81.81(9)
		10	89.46(9)

Table S12. Observed *pseudo*-first order rate constants as a function of nucleophile concentration and chloride concentration in the reaction between $[Au(bpma)Cl]^{2+}$ and L-Cys at pH 2.5 (0.003 M $HClO_4$), 298 K.

λ/nm	10^3 C_{Cl^-}/M	10^3 $C_{L\text{-}Cys}$/M	k_{obsd}/s^{-1}
260	0	2	0.86(9)
		4	1.84(10)
		6	2.79(9)
		8	3.70(9)
		10	4.47(9)
260	25	2	0.98(9)
		4	2.28(10)
		6	3.19(8)
		8	4.05(10)
		10	5.24(9)
260	100	2	0.51(9)
		4	1.23(10)
		6	1.58(9)
		8	2.18(10)
		10	2.67(10)

Table S13. Observed *pseudo*-first order rate constants as a function of nucleophile concentration and chloride concentration in the reaction between $[Au(bpma)Cl]^{2+}$ and L-Met at pH 2.5 (0.003 M $HClO_4$), 298 K.

λ/nm	10^3 C_{Cl^-}/M	10^3 $C_{L\text{-}Met}$/M	k_{obsd}/s^{-1}
260	0	2	0.03(9)
		4	0.05(10)
		6	0.07(9)
		8	0.09(10)
		10	0.11(9)
260	25	2	0.07(9)
		4	0.09(10)
		6	0.12(8)
		8	0.13(10)
		10	0.16(10)
260	100	2	5.79(10)
		4	12.10(10)
		6	15.25(10)
		8	21.04(10)
		10	-

Table S14. Observed *pseudo*-first order rate constants as a function of nucleophile concentration and chloride concentration in the reaction between $[Au(bpma)Cl]^{2+}$ and GSH at pH 2.5 (0.003 M $HClO_4$), 298 K.

λ/nm	10^3 C_{Cl^-}/M	10^3 C_{GSH}/M	k_{obsd}/s^{-1}
300	0	2	0.32(9)
		4	0.48(9)
		6	0.60(9)
		8	0.79(9)
		10	0.96(9)
300	25	2	0.19(9)
		4	0.30(9)
		6	0.51(9)
		8	0.62(9)
		10	0.84(9)
300	100	2	0.13(9)
		4	0.28(9)
		6	0.42(10)
		8	0.54(9)
		10	0.68(10)

Table S15. Observed *pseudo-first* order rate constants as a function of nucleophile concentration and chloride concentration in the reaction between $[Au(bpma)Cl]^{2+}$ and L-Cys at pH 7 (25 mM Hepes buffer), 298 K.

λ/nm	10^3 C_{Cl^-}/M	10^3 $C_{L\text{-}Cys}$/M	k_{obsd}/s^{-1}
250	10	2	6.87(10)
		4	13.18(10)
		6	19.94(10)
		8	27.35(9)
		10	32.58(10)
250	20	2	11.77(10)
		4	20.85(9)
		6	24.31(10)
		8	35.71(9)
		10	44.62(10)

Table S16. Observed *pseudo*-first order rate constants as a function of nucleophile concentration and chloride concentration in the reaction between $[Au(bpma)Cl]^{2+}$ and L-Met at pH 7 (25 mM Hepes buffer), 298 K.

λ/nm	10^3 C_{Cl^-}/M	10^3 $C_{L\text{-}Met}$/M	10^1 k_{obsd}/s^{-1}
260	10	2	0.13(10)
		4	0.18(9)
		6	0.24(10)
		8	0.28(8)
		10	0.34(9)
260	20	2	8.49(10)
		4	17.42(10)
		6	24.36(10)
		8	33.15(9)
		10	41.39(9)

Table S17. Observed *pseudo*-first order rate constants as a function of nucleophile concentration and chloride concentration in the reaction between $[Au(bpma)Cl]^{2+}$ and GSH at pH 7 (25 mM Hepes buffer), 298 K.

λ/nm	10^3 C_{Cl^-}/M	10^3 C_{GSH}/M	k_{obsd}/s^{-1}
300	10	2	0.29(8)
		4	0.45(10)
		6	0.74(10)
		8	0.94(9)
		10	1.14(10)
300	20	2	0.22(10)
		4	0.43(9)
		6	0.71(10)
		8	0.94(9)
		10	1.09(10)

Table S18. Observed *pseudo*-first order rate constants as a function of nucleophile concentration and chloride concentration in the reaction between $[Au(dien)Cl]^{2+}$ and L-Cys at pH 2.5 (0.003 M $HClO_4$), 298 K.

λ/nm	10^3 C_{Cl^-}/M	10^3 $C_{L\text{-}Cys}$/M	k_{obsd}/s^{-1}
300	0	2	0.30(10)
		4	0.48(10)
		6	0.64(10)
		8	0.83(10)
		10	1.00(10)
300	25	2	0.18(10)
		4	0.41(9)
		6	0.62(8)
		8	0.78(10)
		10	0.98(10)
300	100	2	0.16(10)
		4	0.35(9)
		6	0.50(9)
		8	0.69(10)
		10	0.83(10)

Table S19. Observed *pseudo*-first order rate constants as a function of nucleophile concentration and chloride concentration in the reaction between $[Au(dien)Cl]^{2+}$ and L-Met at pH 2.5 (0.003 M $HClO_4$), 298 K.

λ/nm	10^3 C_{Cl^-}/M	10^3 $C_{L\text{-}Met}$/M	k_{obsd}/s^{-1}
270	0	2	0.79(10)
		4	0.99(9)
		6	1.10(9)
		8	1.26(10)
		10	1.43(9)

Table S20. Observed *pseudo*-first order rate constants as a function of nucleophile concentration and chloride concentration in the reaction between $[Au(dien)Cl]^{2+}$ and GSH at pH 2.5 (0.003 M $HClO_4$), 298 K.

λ/nm	10^3 C_{Cl^-}/M	10^3 C_{GSH}/M	k_{obsd}/s^{-1}
300	0	2	0.16(10)
		4	0.23(9)
		6	0.31(10)
		8	0.35(10)
		10	0.45(10)
300	25	2	0.13(10)
		4	0.17(9)
		6	0.22(10)
		8	0.28(10)
		10	0.33(10)
300	100	2	0.06(10)
		4	0.13(9)
		6	0.17(8)
		8	0.24(10)
		10	0.29(10)

Table S21. Observed *pseudo*-first order rate constants as a function of nucleophile concentration and chloride concentration in the reaction between $[Au(dien)Cl]^{2+}$ and L-Cys at pH 7 (25 mM Hepes buffer), 298 K.

λ/nm	10^3 C_{Cl^-}/M	10^3 $C_{L\text{-}Cys}$/M	k_{obsd}/s^{-1}
300	0	2	13.57(10)
		4	24.51(9)
		6	33.27(9)
		8	43.40(9)
		10	50.54(10)
300	10	2	19.37(9)
		4	30.35(9)
		6	44.33(10)
		8	57.05(10)
		10	71.60(10)

Table S22. Observed *pseudo*-first order rate constants as a function of nucleophile concentration and chloride concentration in the reaction between $[Au(dien)Cl]^{2+}$ and L-Met at pH 7 (25 mM Hepes buffer), 298 K.

λ/nm	10^3 C_{Cl^-}/M	10^3 $C_{L\text{-}Met}$/M	k_{obsd}/s^{-1}
255	0	2	0.21(10)
		4	0.34(9)
		6	0.49(9)
		8	0.63(9)
		10	0.77(9)
260	10	2	1.31(9)
		4	1.64(9)
		6	1.91(9)
		8	2.07(9)
		10	2.24(8)

Table S23. Observed *pseudo*-first order rate constants as a function of nucleophile concentration and chloride concentration in the reaction between $[Au(dien)Cl]^{2+}$ and GSH at pH 7 (25 mM Hepes buffer), 298 K.

λ/nm	10^3 C_{Cl^-}/M	10^3 C_{GSH}/M	k_{obsd}/s^{-1}
300	0	2	6.67(10)
		4	8.75(10)
		6	10.98(9)
		8	12.44(9)
		10	13.42(10)
300	10	2	9.13(10)
		4	11.89(10)
		6	14.36(9)
		8	16.12(8)
		10	18.59(10)

Table S24. Crystal data and structure refinement for [Au(terpy)Cl]$(ClO_4)_2$.

CCDC - 967806	
Empirical formula	$C_{15}H_{11}AuCl_3N_3O_8$
Formula weight	664.58
Temperature	120(2) K
Wavelength	0.71073 Å
Crystal system, space group	Monoclinic, $P2_1$ (no. 4)
Unit cell dimensions	a = 8.2269(8) Å α = 90 ° b = 13.7017(14) Å β = 98.288(2) ° c = 8.3555(8) Å γ = 90 °
Volume	932.02(16) $Å^3$
Z, Calculated density	2, 2.368 Mg/m^3
Absorption coefficient	8.376 mm^{-1}
F(000)	632
Crystal size	0.12 x 0.05 x 0.03 mm
Theta range for data collection	2.46 to 29.60 °
Limiting indices	-11<=h<=11, -18<=k<=19, -11<=l<=11
Reflections collected / unique	18859 / 5201 [R_{int} = 0.0352]
Completeness to theta = 29.60	100.0 %
Absorption correction	Semi-empirical from equivalents
Max. and min. transmission	0.746 and 0.605
Refinement method	Full-matrix least-squares on F^2
Data / restraints / parameters	5201 / 1 / 272
Goodness-of-fit on F^2	0.990

Final *R* indices [$I>2\sigma(I)$]	R_1 = 0.0212, wR_2 = 0.0413
R indices (all data)	R_1 = 0.0259, wR_2 = 0.0429
Absolute structure parameter	0.302(5)
Largest diff. peak and hole	1.064 and -0.746 e·Å^{-3}

Table S25. Selected bond distances [Å] and bond angles [°][Au(terpy)Cl]$(ClO_4)_2$ with e.s.d's in parentheses.

Bond distances [Å]		Bond angles [°]	
Au(1)-N(1)	2.015(5)	N(2)-Au(1)-N(1)	81.4(2)
Au(1)-N(2)	1.957(5)	N(2)-Au(1)-N(3)	81.9(2)
Au(1)-N(3)	2.022(4)	N(1)-Au(1)-N(3)	163.3(2)
Au(1)-Cl(1)	2.251(2)	N(2)-Au(1)-Cl(1)	179.0(2)
		N(1)-Au(1)-Cl(1)	97.9(2)
		N(3)-Au(1)-Cl(1)	98.8(2)

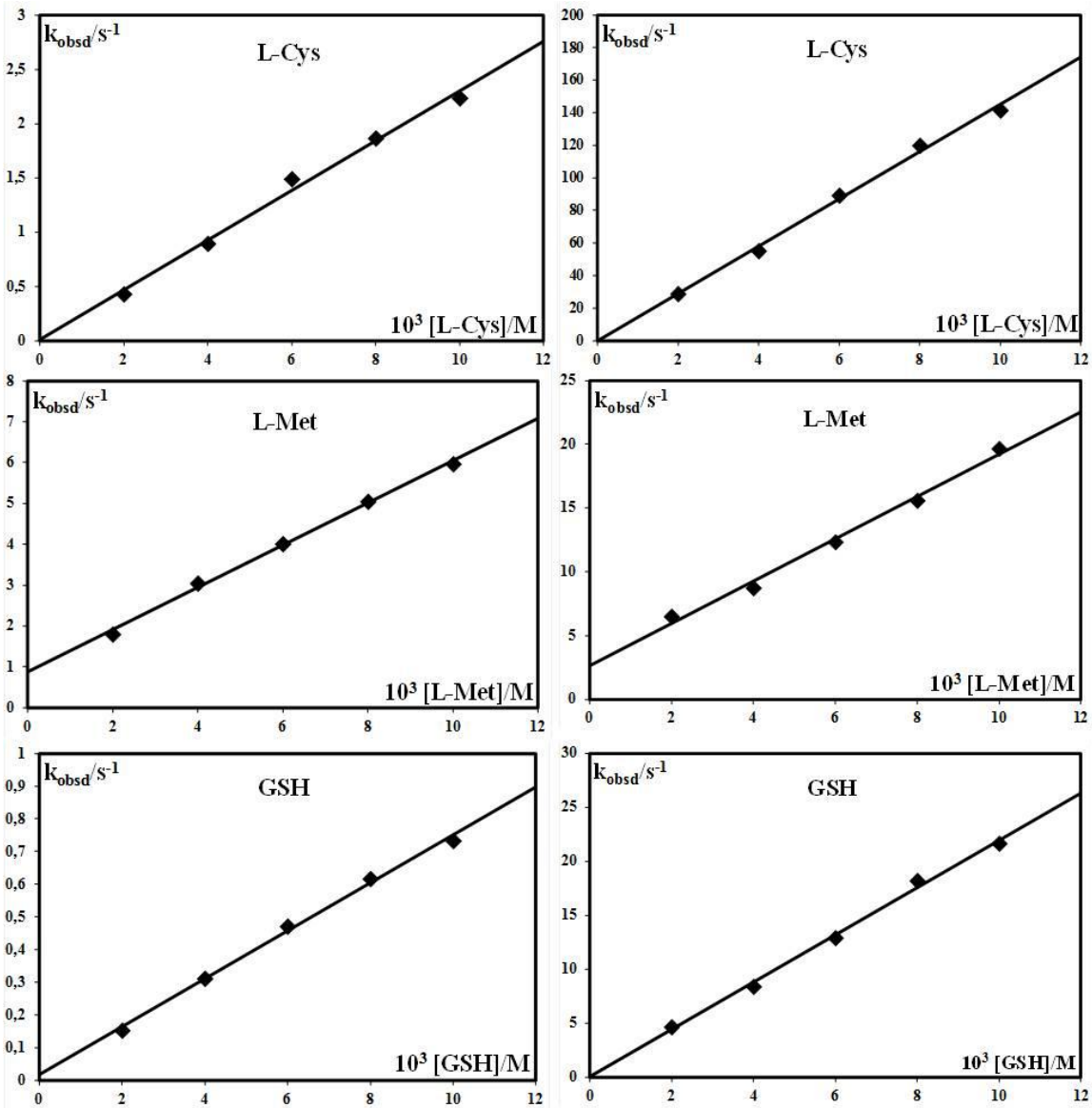

Figure S1. *Pseudo*-first-order rate constants plotted as a function of nucleophile concentration for the substitution reactions of the $[AuCl_4]^-$ complex by L-Cys, L-Met and GSH at pH 7 (0.1 M $NaClO_4$), without added chloride (left), in the presence of 10 mM chloride (right), at 298 K.

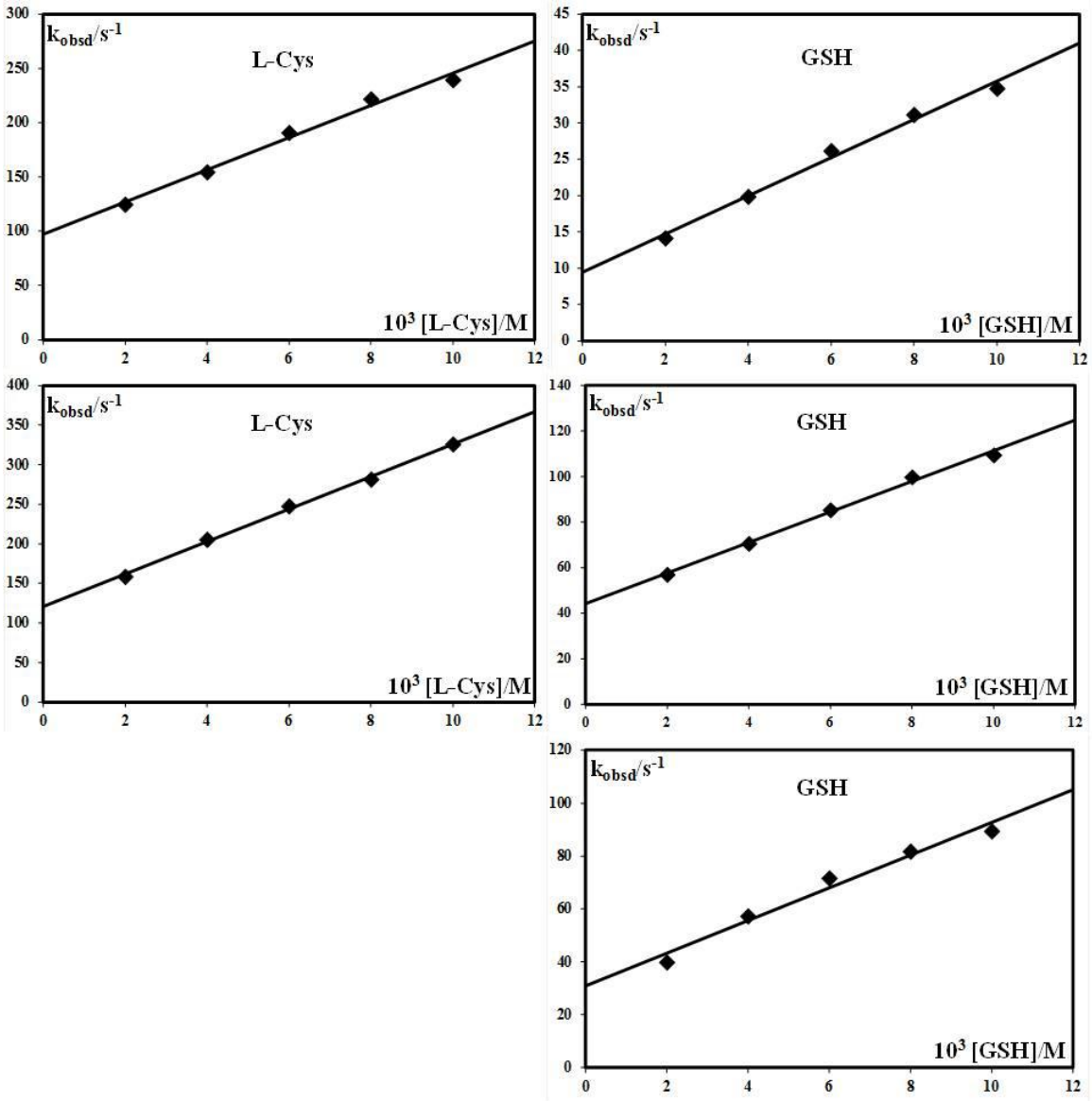

Figure S2. *Pseudo*-first-order rate constants plotted as a function of nucleophile concentration for the substitution reactions of the $[Au(terpy)Cl]^{2+}$ complex with L-Cys and GSH at pH 7 (25 mM Hepes buffer), without added chloride (first line), in the presence of 10 mM (second line) and 100 mM chloride (third line), at 298 K.

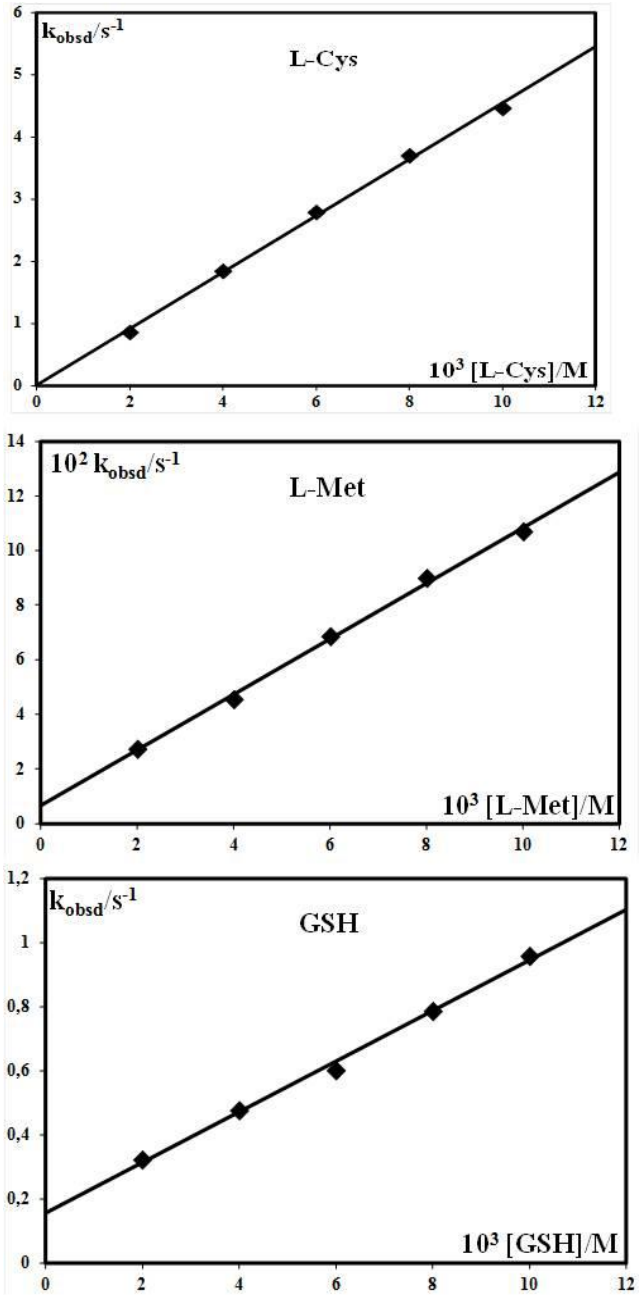

Figure S3. *Pseudo*-first-order rate constants plotted as a function of nucleophile concentration for the substitution reactions of the $[Au(bpma)Cl]^{2+}$ complex with L-Cys, L-Met and GSH at pH 2.5 (0.003 M $HClO_4$), without added chloride, at 298 K.

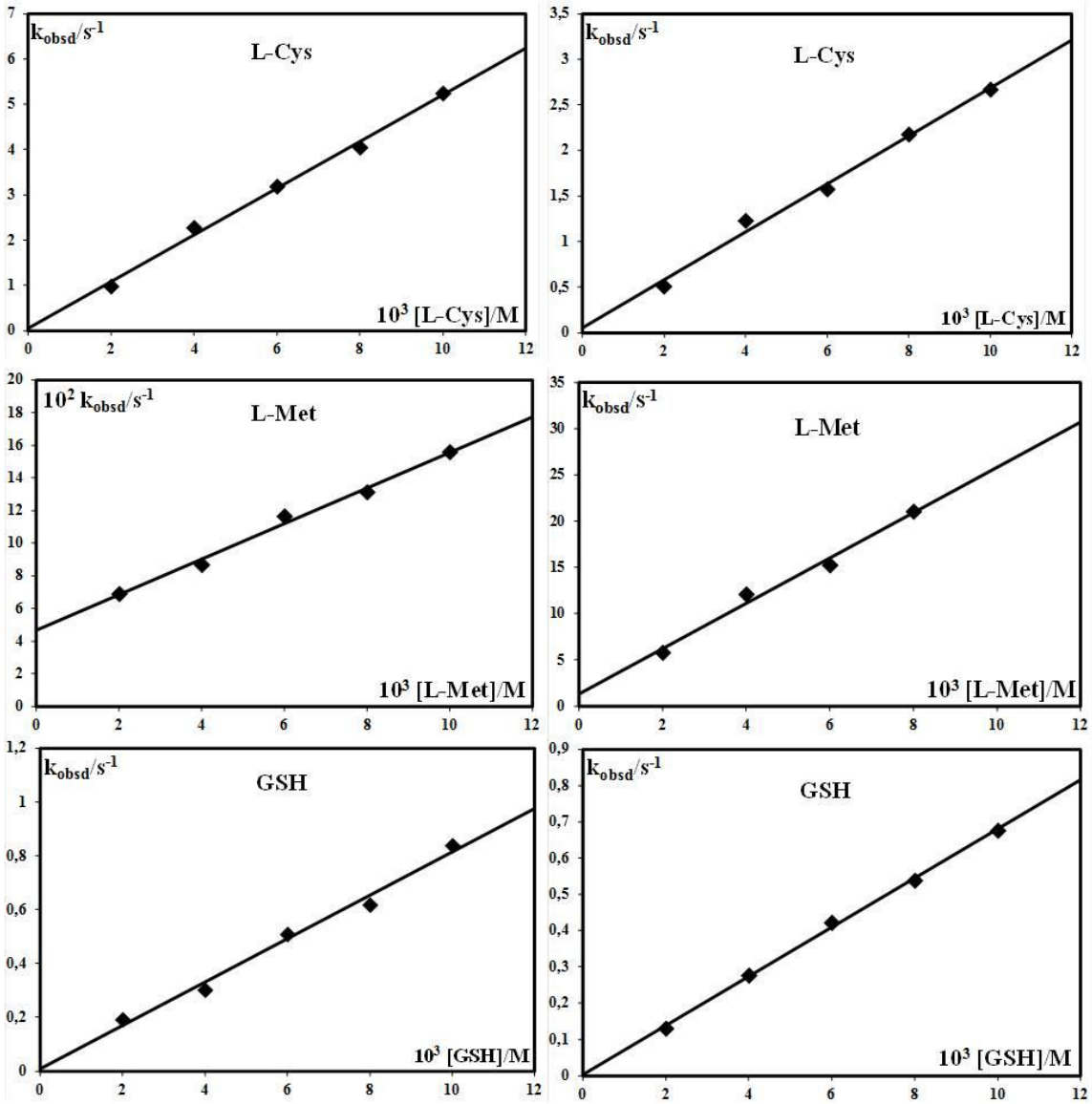

Figure S4. *Pseudo*-first-order rate constants plotted as a function of nucleophile concentration for the substitution reactions of the $[Au(bpma)Cl]^{2+}$ complex with L-Cys, L-Met and GSH at pH 2.5 (0.003 M $HClO_4$), in the presence of 25 mM (left) and 100 mM chloride (right), at 298 K.

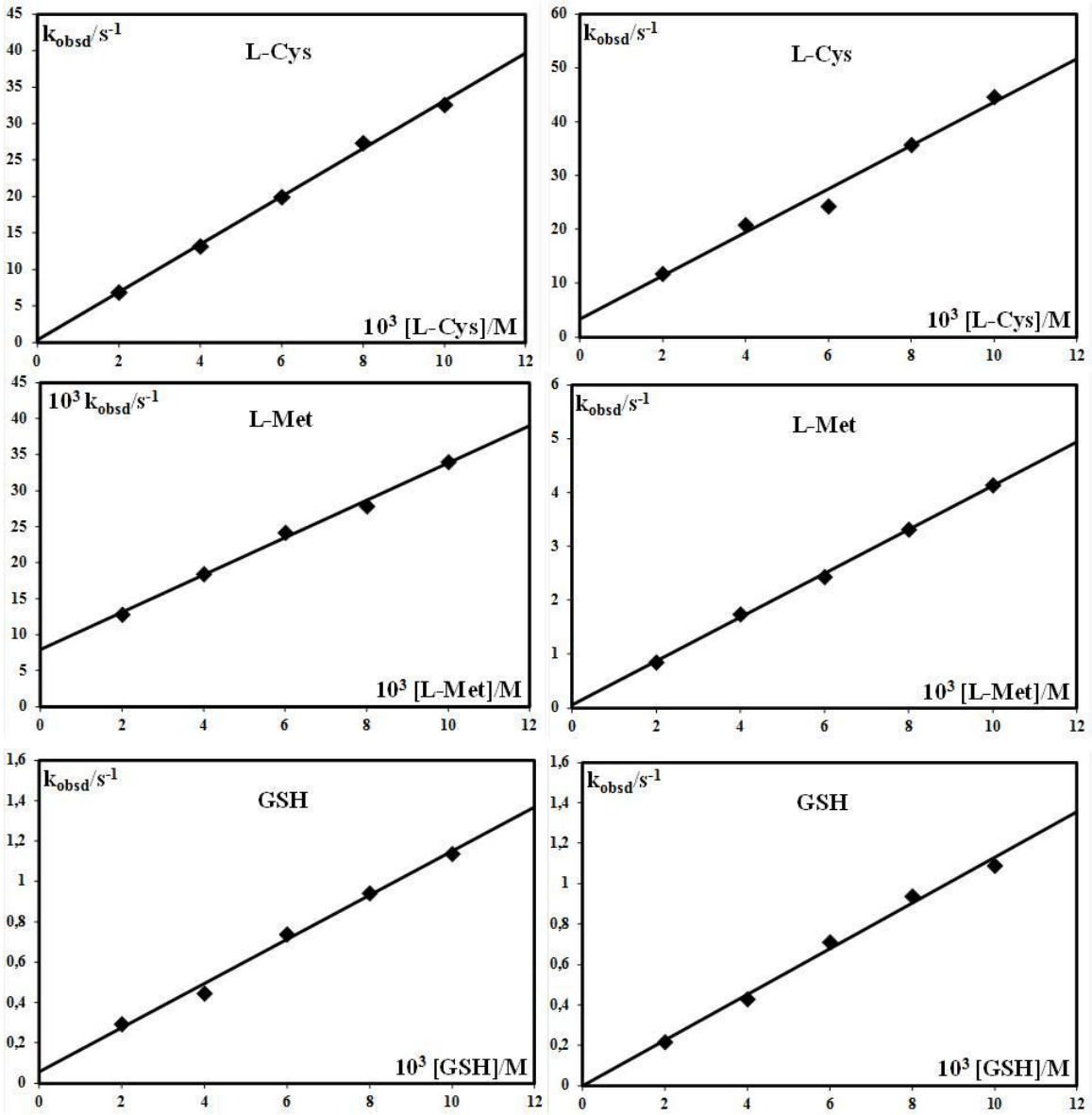

Figure S5. *Pseudo*-first-order rate constants plotted as a function of nucleophile concentration for the substitution reactions of the $[Au(bpma)Cl]^{2+}$ complex with L-Cys, L-Met and GSH at pH 7 (25 mM Hepes buffer), in the presence of 10 mM (left) and 20 mM chloride (right), at 298 K.

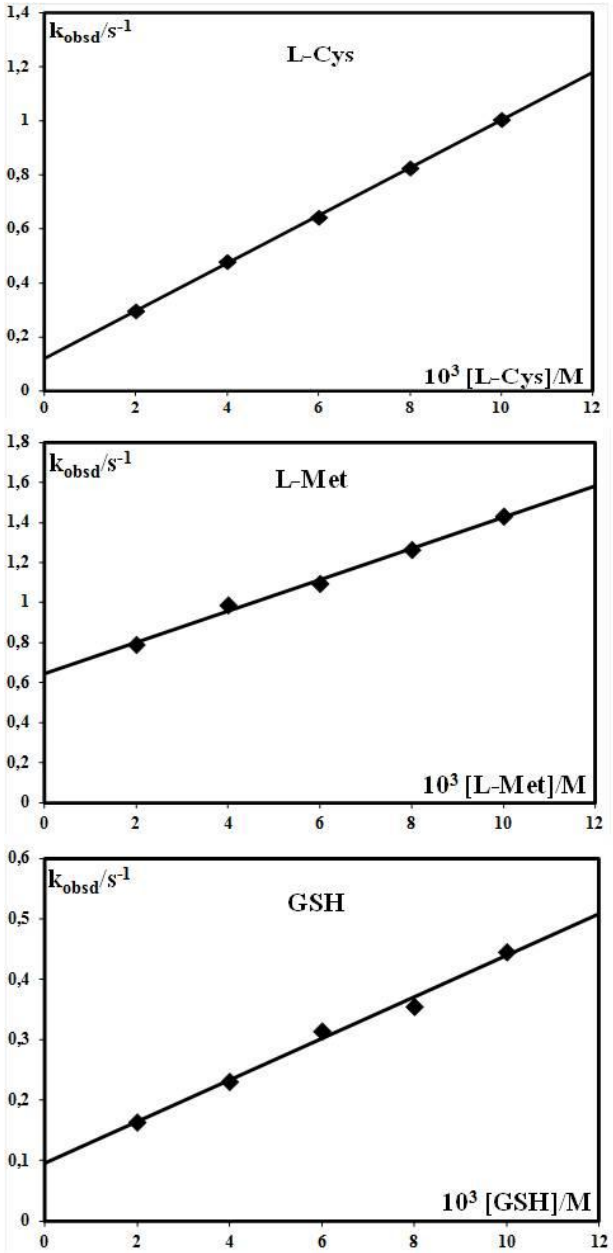

Figure S6. *Pseudo*-first order rate constants plotted as a function of nucleophile concentration for the substitution reactions of the $[Au(dien)Cl]^{2+}$ complex with L-Cys, L-Met and GSH at pH 2.5 (0.003 M $HClO_4$), without added chloride, at 298 K.

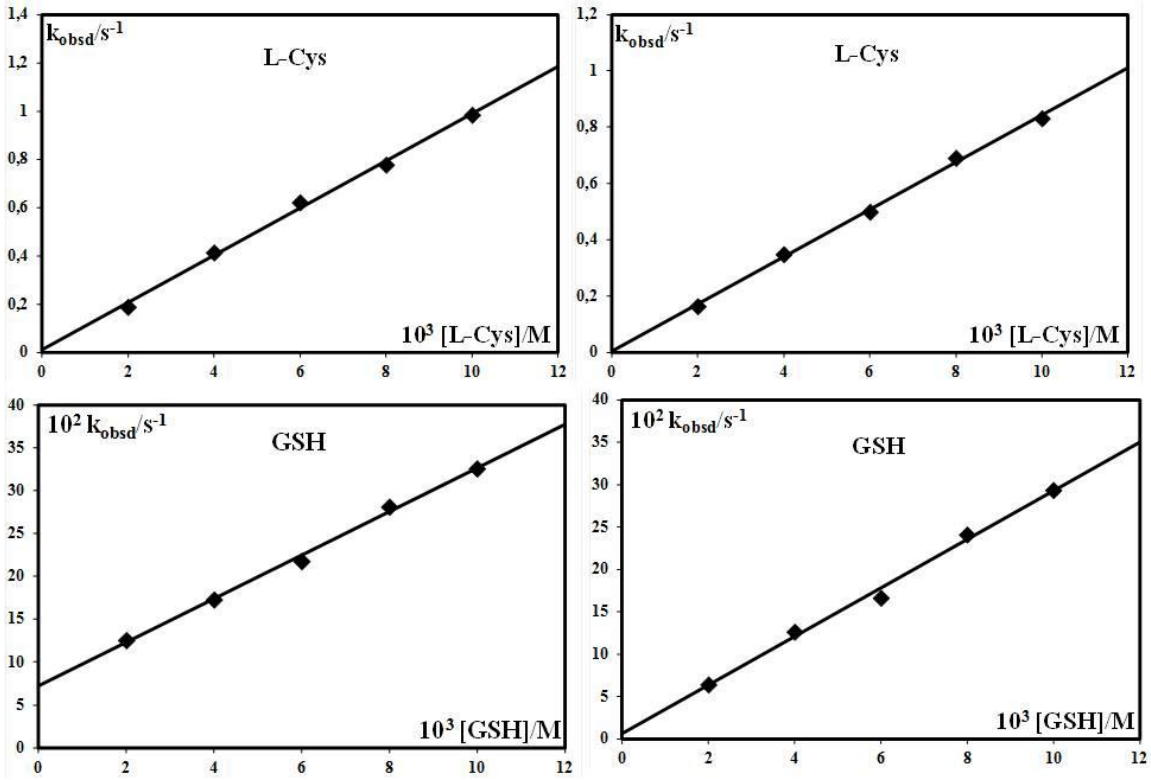

Figure S7. *Pseudo*-first-order rate constants plotted as a function of nucleophile concentration for the substitution reactions of the $[Au(dien)Cl]^{2+}$ complex with L-Cys and GSH at pH 2.5 (0.003 M $HClO_4$), in the presence of 25 mM (left) and 100 mM chloride (right), at 298 K.

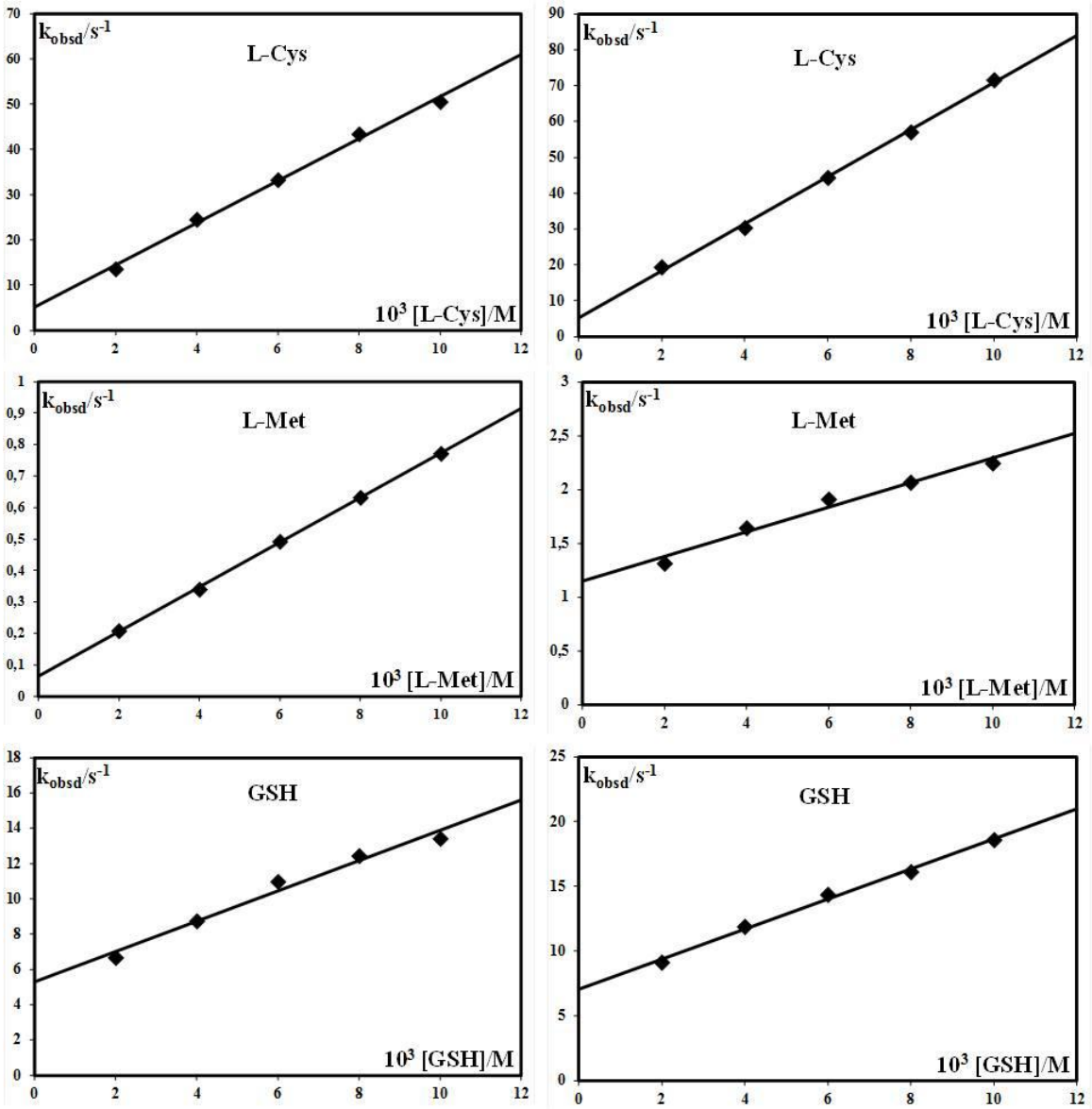

Figure S8. *Pseudo*-first-order rate constants plotted as a function of nucleophile concentration for the substitution reactions of the $[Au(dien)Cl]^{2+}$ complex with L-Cys, L-Met and GSH at pH 7 (25 mM Hepes buffer), without excess of chloride (left), in the presence of 10 mM chloride (right), at 298 K.

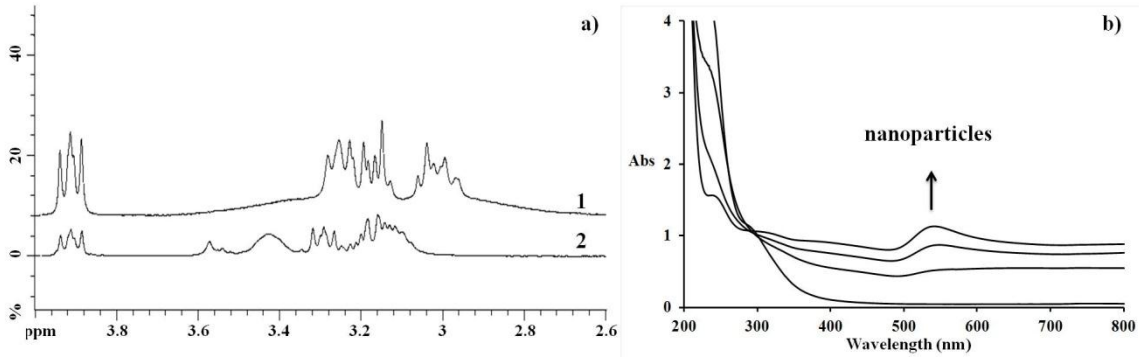

Figure S9. Spectra of 2×10^{-4} M $[AuCl_4]^-$ in 25 mM Hepes buffer solution;
a) ^{1}H NMR spectra as an indication of the oxidation of Hepes: 1- Hepes Buffer; 2- oxidized Hepes buffer, recorded after 30 min
b) UV-Vis spectrum as an indication of gold nanoparticles formation, recorded during 30 min.

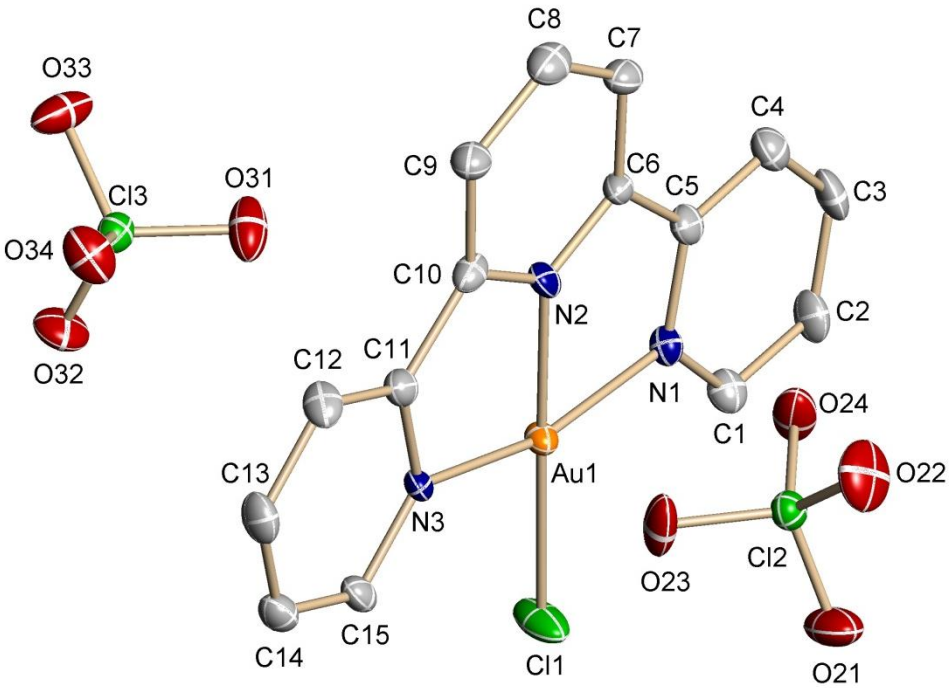

Figure S10. The crystal structure of the complex [Au(terpy)Cl]$(ClO_4)_2$ with the applied numbering scheme (50 % probability ellipsoids, hydrogen atoms omitted for clarity).

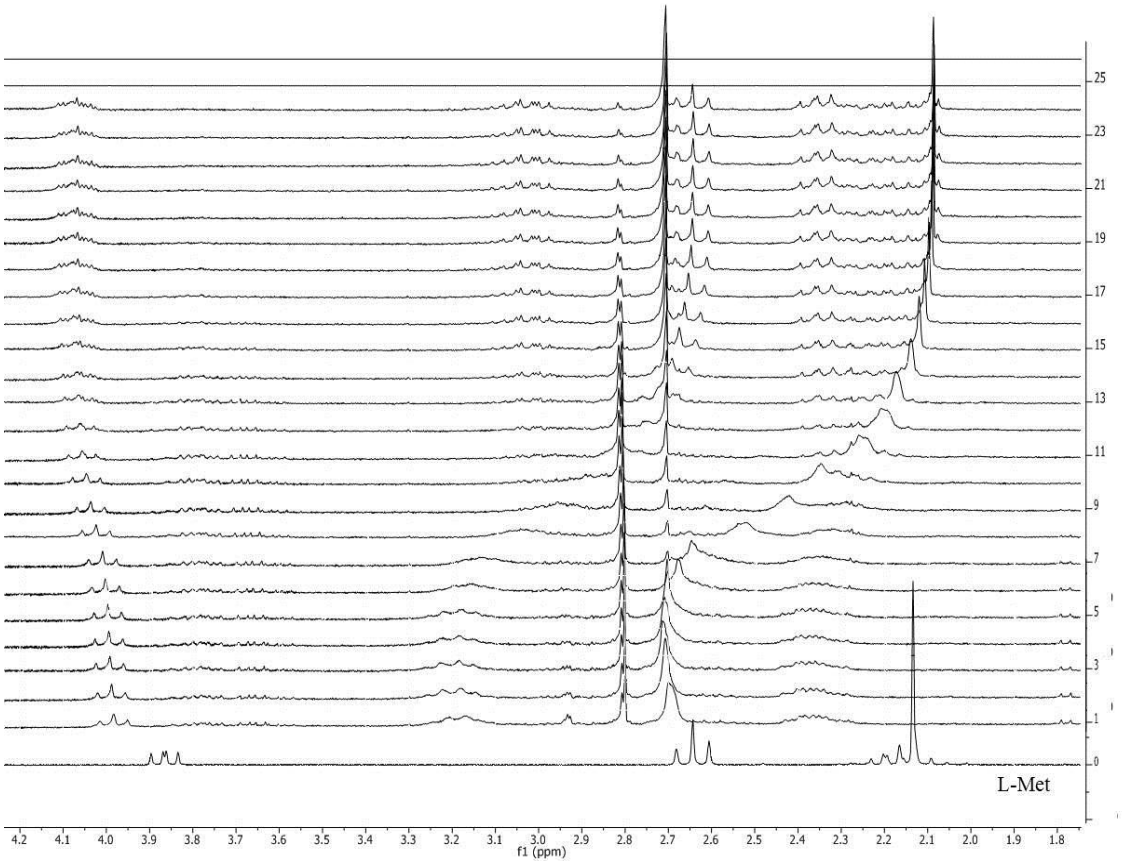

Figure S11. ^{1}H NMR spectra recorded overnight for the reaction between an equimolar amount of $[AuCl_4]^-$ and L-Met in D_2O, compared to the spectrum of L-Met.

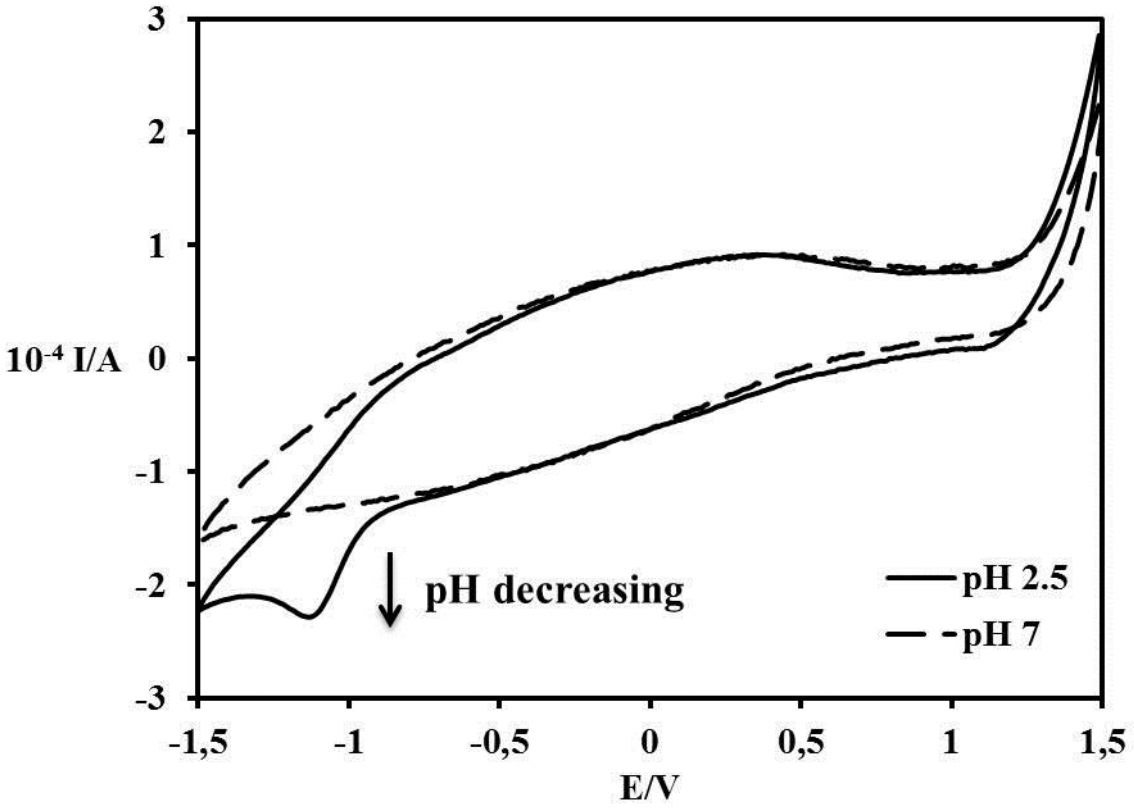

Figure S12. Cyclic voltammograms obtained for the background electrolyte, 0.4 M NaCl aqueous solution (pH 7) and in the presence of 0.003 M HCl (pH 2.5).

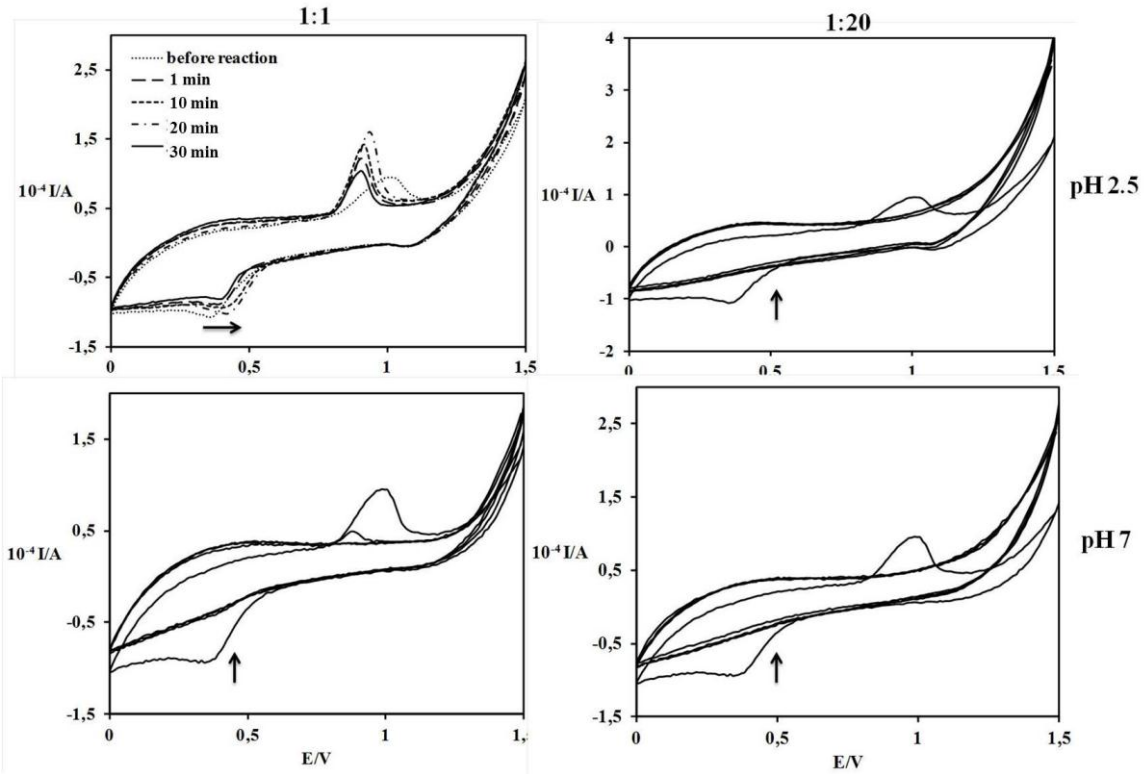

Figure S13. Cyclic voltammograms recorded during the reaction of $[AuCl_4]^-$ with L-Cys, at different complex to L-Cys molar ratio and two pH values; GC electrode, scan rate 0.1 Vs^{-1}, E_{step} = 0.01 V, 0.4 M NaCl as background electrolyte.

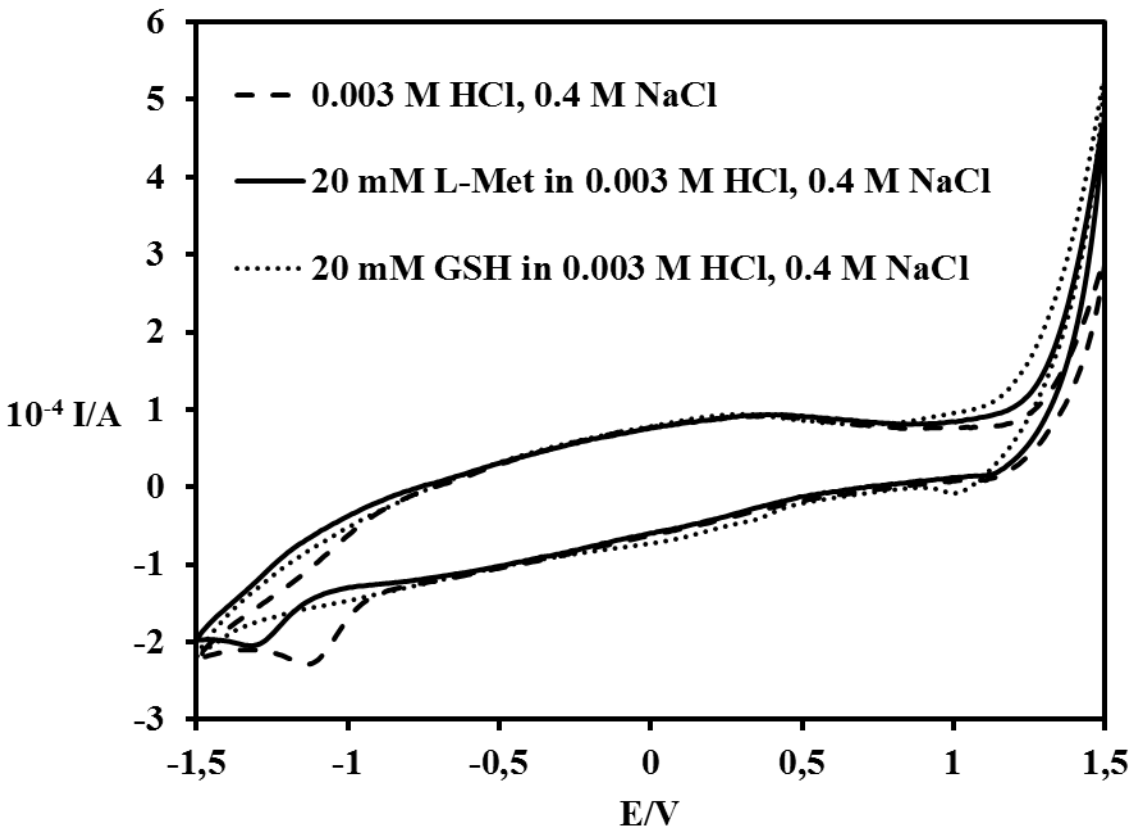

Figure S14. Cyclic voltammograms recorded for the background electrolyte (0.003 M HCl in 0.4 M NaCl) and in the presence of 20 mM Met or GSH; scan rate 0.1 Vs^{-1}, E_{step} = 0.01 V.

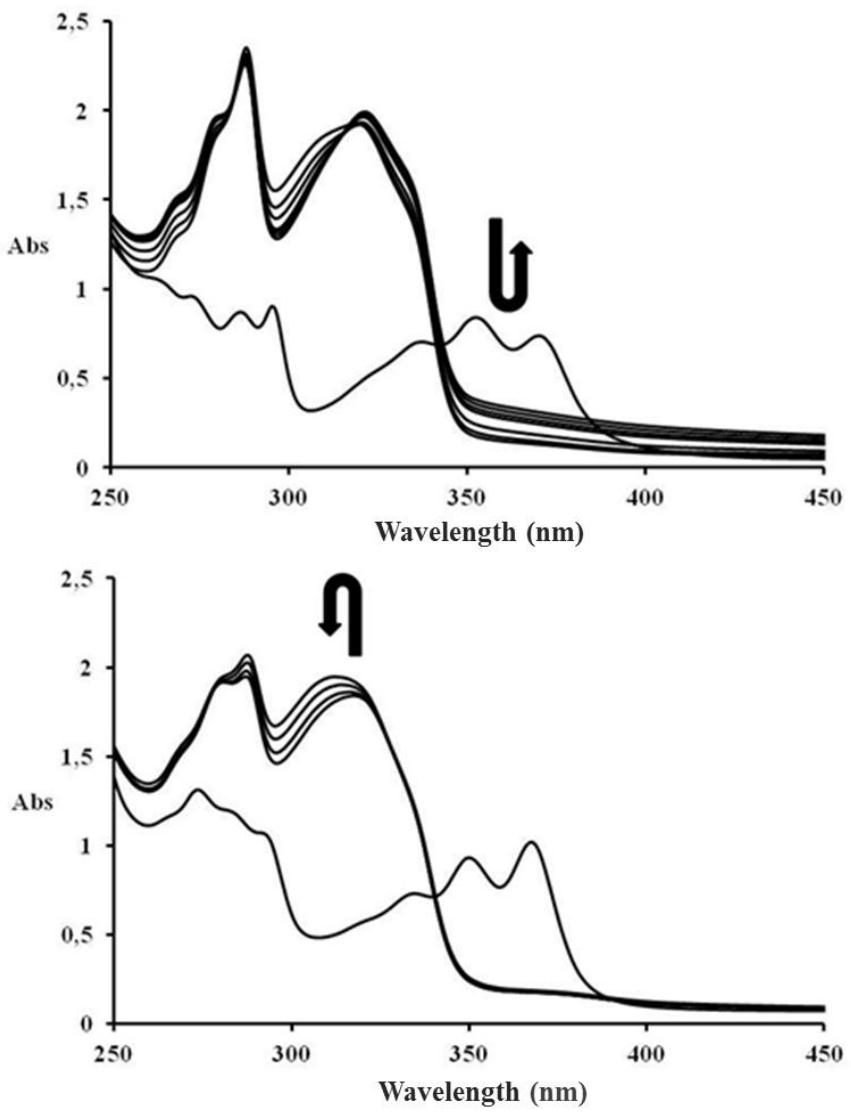

Figure S15. UV-Vis spectra recorded for the reaction of 1×10^{-4} M $[Au(terpy)Cl]^{2+}$ and 1×10^{-2} M GSH in aqueous solution, without added chloride ions, at pH 2.5 (top) and at pH 7 (bottom); evidence for further disulfide bond oxidation.

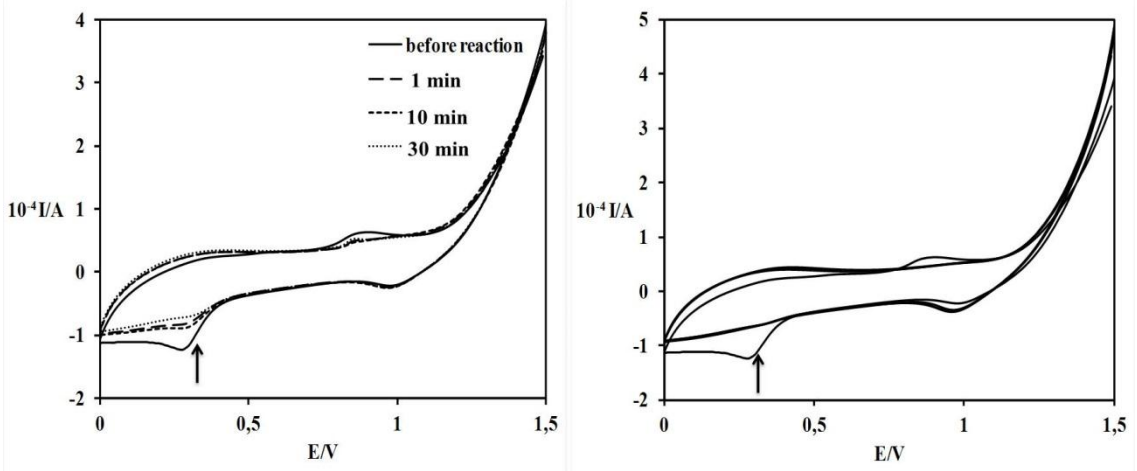

Figure S16. Cyclic voltammograms obtained for the reaction of $[AuCl_4]^-$ with GSH, in the molar ratio 1:1 - left, 1:20 - right, at pH 2.5; GC electrode, scan rate 0.1 Vs^{-1}, 0.4 M NaCl as background electrolyte.

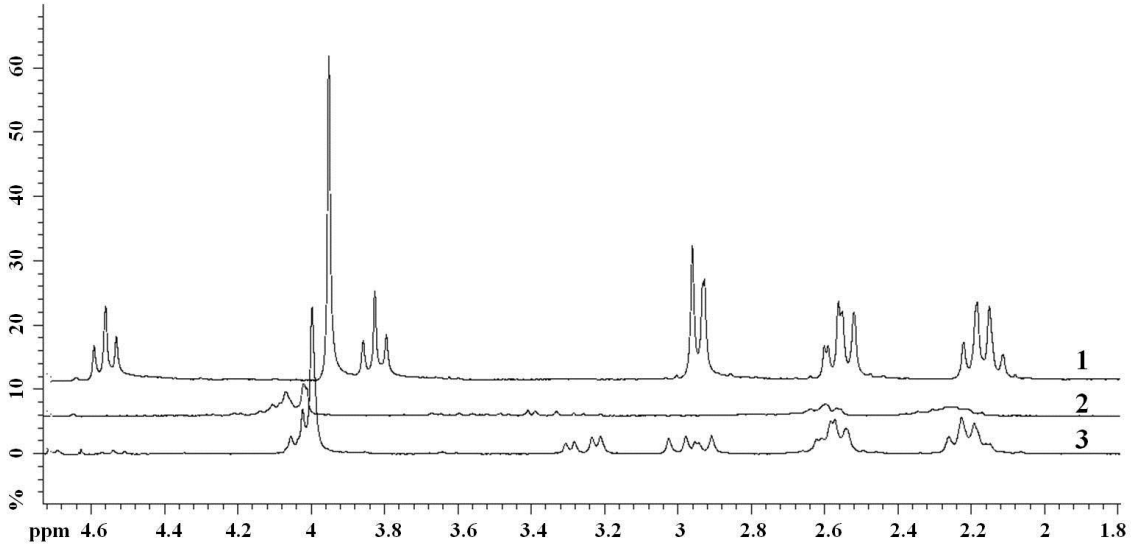

Figure S17. Comparison of the ^1H NMR spectra recorded for: 1) GSH; 2) the reaction of an equimolar amount of $[AuCl_4]^-$ and GSH; 3) the reaction of 10 mM $[AuCl_4]^-$ and 30 mM GSH; 0.4 M NaCl in D_2O; 15 min.

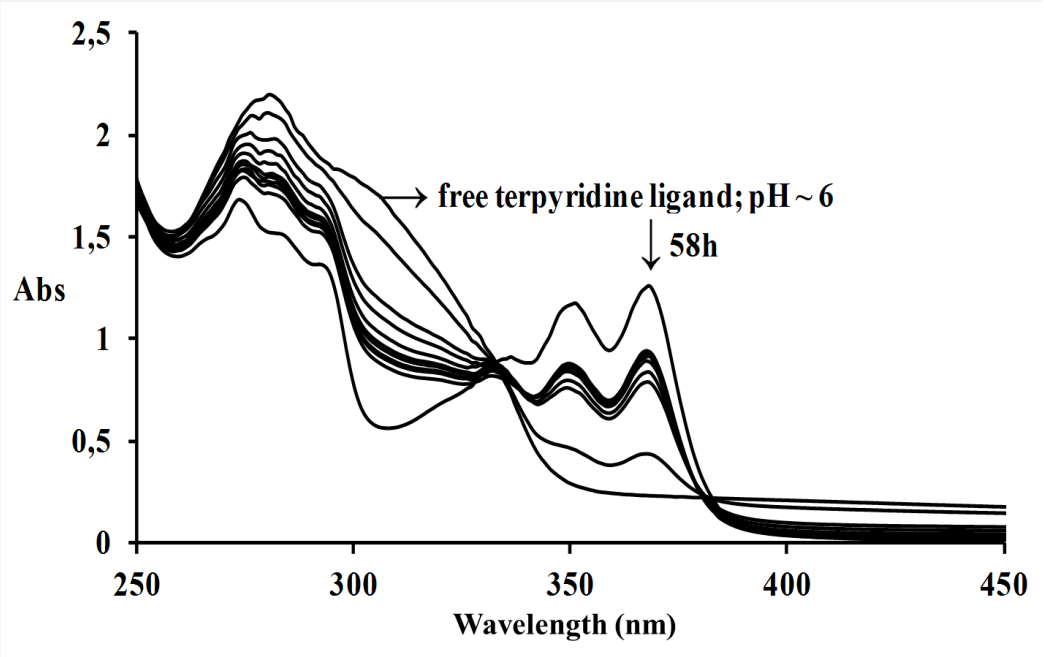

Figure S18. Spectra of the absorption changes recorded during the reaction of $[Au(terpy)Cl]^{2+}$ and L-Cys in the molar ratio 2:1 in 25 mM Hepes buffer over 58 h.

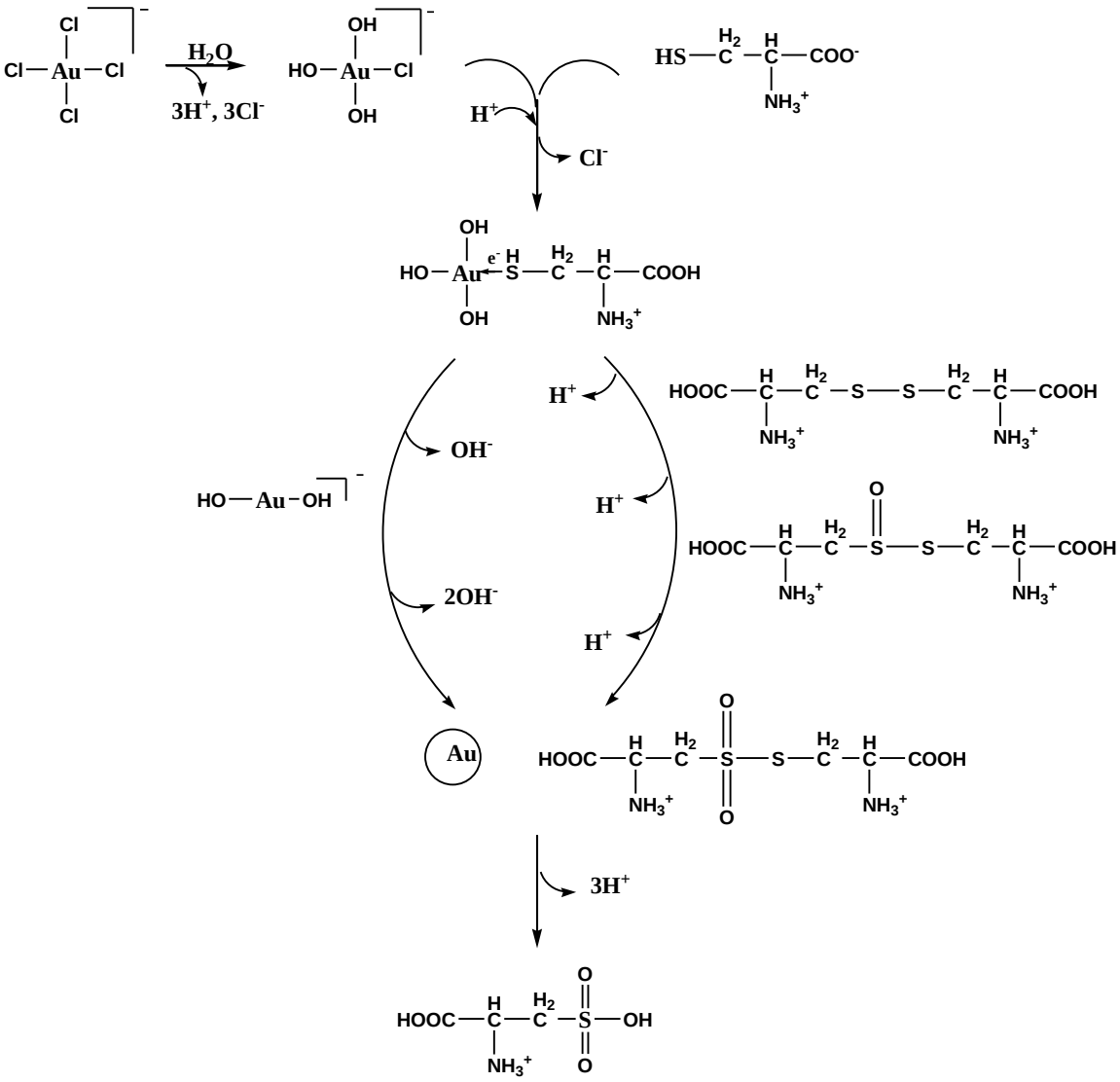

Scheme S1. Schematic presentation of the proposed mechanism for the reaction of $[AuCl_4]^-$ and L-Cys with formation of intermediate and final products.